Chapter 3

SIMULATION OF HENs

This chapter describes how dynamic simulations of HENs can be carried out. The type and complexity of the model of each heat exchanger significantly affect the efforts required for HEN simulation, and focus is on the development of a general heat exchanger model that simplifies the simulations. Some fundamentals of heat transfer and steady state properties of ideal countercurrent heat exchangers are briefly described, and the chapter closes by explaining how dynamic simulation of controlled HENs are performed.

3.1 Governing equations for heat transfer

A quite general expression for the energy balance (e.g. Bird *et al*., 1960), using cartesian tensor notation, is

$$\underbrace{\frac{\partial}{\partial t}\left(\rho\hat{E}\right)}_{\text{Accumulation}} + \underbrace{\frac{\partial}{\partial x_i}\left(\rho u_i \hat{E}\right)}_{\text{Convection}} = \underbrace{\frac{\partial}{\partial x_i}\left(\alpha\frac{\partial \hat{E}}{\partial x_i}\right)}_{\text{Diffusion}} + S \tag{3.1}$$

where $\hat{E}$ is specific energy (mass basis) and u_i are the velocity components in the three spatial directions, x_i. It is assumed that the heat transfer due to diffusion is given by Fourier's law.

$$q_i = -k\frac{\partial T}{\partial u_i} \tag{3.2}$$

Here, k is the *thermal conductivity* of the material, and the *thermal diffusivity* α in equation (3.1) is given by $\alpha = k/c_v$. Equation (3.1) gives the specific energy at any point within arbitrary system boundaries. The source term S denotes energy flow across the system boundaries, and it may also include heat transfer not included in the other terms, such as radiation. Equation (3.1), together with similar expressions for conservation of mass and impulse, may be used for detailed studies of heat exchangers to investigate for instance different geometries inside the unit, see e.g. Sha *et al.* (1982). The governing equation (3.1) may also be used to derive simplified expressions for various cases. We shall approach modeling of heat exchangers by setting up energy balances for the idealized countercurrent configuration shown below, and see that the result conforms to a simplified version of equation (3.1).

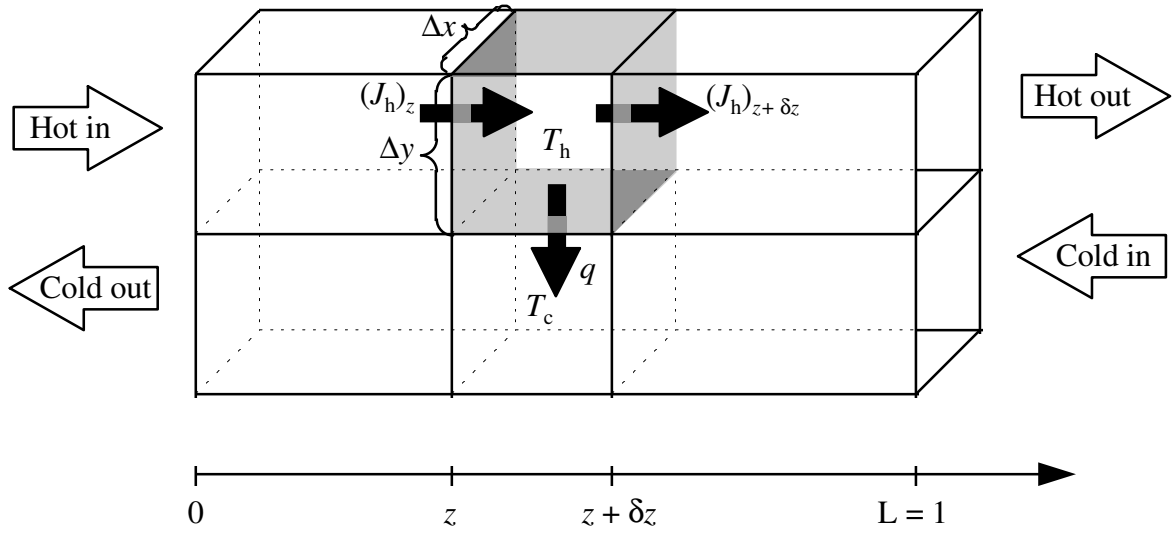

Figure 3.1 Sketch of ideal countercurrent heat exchange.

Heat q is transferred from the hot to the cold stream through the wall with an assumed constant heat transfer coefficient U. First, consider the hot side, where the density ρ_h and the mass flux J_h are assumed constant. There are no temperature gradients in the crosswise directions, and diffusion of energy is assumed negligible (compared to convection) in the streamwise direction z. Also, mechanical energy is assumed small, thus the dynamic equation for thermal energy in the hot control volume indicated in figure 3.1 becomes

$$\frac{d}{dt}\left(\rho_h \Delta x \Delta y \delta z \hat{E}_h^U\right) = \left(J_h \Delta x \Delta y \hat{E}_h^U\right)_z - \left(J_h \Delta x \Delta y \hat{E}_h^U\right)_{z+\delta z} - \underbrace{U \Delta x \delta z (T_h - T_c)}_{q} \tag{3.3}$$

$\hat{E}_h^U$ is the specific internal energy in the hot side control volume. Rearranging somewhat and letting δz approach zero, we get

$$\underbrace{\frac{\partial}{\partial t}\left(\rho_h \hat{E}_h^U\right)}_{\text{Accumulation}} + \underbrace{J_h \frac{\partial \hat{E}_h^U}{\partial z}}_{\text{Convection}} = \underbrace{-\frac{U}{\Delta y}(T_h - T_c)}_{\text{Source}} \tag{3.4}$$

This is identical to equation (3.1) in one dimension (z-direction). Note that for the convective term, we have $J_h = \rho_h u_z$ where both the density and the z-direction velocity u_z are constants. Also, the diffusive term is zero in equation (3.4) since this was assumed negligible compared to the convective term. The source term is the heat transferred into the system across the boundaries. For the hot side, the source term is negative since heat is transferred from the hot to the cold stream. Now, we introduce the specific heat capacity

$$c_v = \left(\frac{\partial E^U}{\partial T} \right)_v \tag{3.5}$$

The assumption of incompressible fluids leads to $c_v = c_p$ and the heat capacity flowrate will be defined as $CP = \rho F c_v$, and terms related to pressure work are neglected. With the definition of c_v, the equation describing the temperature $T_h = T_h(t,z)$ in the hot side of the idealized heat exchanger is obtained. The corresponding equation for the cold side is derived similarly, and this yields two coupled partial differential equations

$$\frac{\partial T_h}{\partial t} + \frac{F_h L}{V_h} \frac{\partial T_h}{\partial z} = -\frac{UA}{\rho_h V_h c_{v,h}} (T_h - T_c) \tag{3.6}$$

$$\frac{\partial T_c}{\partial t} - \frac{F_c L}{V_c} \frac{\partial T_c}{\partial z} = \frac{UA}{\rho_c V_c c_{v,c}} (T_h - T_c) \tag{3.7}$$

In these equations, A is the total heat exchanging area, F_h and F_c are volumetric flowrates on hot and cold side, and V_h and V_c are total volumes of hot and cold side. The total length, L, is equal to unity in figure 3.1, and this implies that z is dimensionless. Equations (3.6) and (3.7) form *one* basis for modeling of heat exchangers. In the next section it will be shown that discretizing these equations in the spatial direction (z-direction) may lead to exactly the same set of equations as when the mixing tank concept is used as basis. The remaining part of this section will concern some basic steady state properties of ideal countercurrent heat exchange. At steady state and when introducing the number of transfer units $NTU_h = UA/CP_h$ and $NTU_c = UA/CP_c$ (where $CP_h = \rho_h F_h c_{v,h}$ and $CP_c = \rho_c F_c c_{v,c}$), equations (3.6) and (3.7) may be written as

$$\frac{d}{dz} \begin{bmatrix} T_h \\ T_c \end{bmatrix} = \begin{bmatrix} -NTU_h & NTU_h \\ -NTU_c & NTU_c \end{bmatrix} \begin{bmatrix} T_h \\ T_c \end{bmatrix} \tag{3.8}$$

Using the inlet temperatures as boundary conditions:

$$T_h(z = 0) = T_{h,in} \tag{3.9}$$

$$T_c(z = 1) = T_{c,in} \tag{3.10}$$

the solution to equation (3.8) is given by the two following equations:

$$T_{\mathrm{h}}(z) = T_{\mathrm{h,in}} - \frac{NTU_{\mathrm{h}}\left(1 - e^{(NTU_{\mathrm{c}} - NTU_{\mathrm{h}})z}\right)}{NTU_{\mathrm{h}} - NTU_{\mathrm{c}} e^{(NTU_{\mathrm{c}} - NTU_{\mathrm{h}})}}\left(T_{\mathrm{h,in}} - T_{\mathrm{c,in}}\right) \tag{3.11}$$

$$T_{\mathrm{c}}(z) = T_{\mathrm{c,in}} - \frac{NTU_{\mathrm{c}}\left(e^{(NTU_{\mathrm{c}} - NTU_{\mathrm{h}})} - e^{(NTU_{\mathrm{c}} - NTU_{\mathrm{h}})z}\right)}{NTU_{\mathrm{h}} - NTU_{\mathrm{c}} e^{(NTU_{\mathrm{c}} - NTU_{\mathrm{h}})}}\left(T_{\mathrm{h,in}} - T_{\mathrm{c,in}}\right) \tag{3.12}$$

These equations show that the temperature through an ideal heat exchanger is a nonlinear function of the position z. The outlet temperatures are given by

$$T_{\mathrm{h,out}} = T_{\mathrm{h}}(z=1) = T_{\mathrm{h,in}} - \frac{NTU_{\mathrm{h}}\left(1 - e^{(NTU_{\mathrm{c}} - NTU_{\mathrm{h}})}\right)}{\underbrace{NTU_{\mathrm{h}} - NTU_{\mathrm{c}} e^{(NTU_{\mathrm{c}} - NTU_{\mathrm{h}})}}_{P_{\mathrm{h}}}}\left(T_{\mathrm{h,in}} - T_{\mathrm{c,in}}\right) \tag{3.13}$$

$$T_{\mathrm{c,out}} = T_{\mathrm{c}}(z=0) = T_{\mathrm{c,in}} + \frac{NTU_{\mathrm{c}}\left(1 - e^{(NTU_{\mathrm{c}} - NTU_{\mathrm{h}})}\right)}{\underbrace{NTU_{\mathrm{h}} - NTU_{\mathrm{c}} e^{(NTU_{\mathrm{c}} - NTU_{\mathrm{h}})}}_{P_{\mathrm{c}}}}\left(T_{\mathrm{h,in}} - T_{\mathrm{c,in}}\right) \tag{3.14}$$

where the thermal efficiencies P_{h} and P_{c} are introduced. These are *defined* as

$$P_{\mathrm{h}} = \frac{T_{\mathrm{h,in}} - T_{\mathrm{h,out}}}{T_{\mathrm{h,in}} - T_{\mathrm{c,in}}} \tag{3.15}$$

$$P_{\mathrm{c}} = \frac{T_{\mathrm{c,out}} - T_{\mathrm{c,in}}}{T_{\mathrm{h,in}} - T_{\mathrm{c,in}}} \tag{3.16}$$

The definitions of thermal efficiencies apply for all flow configurations. One physical interpretation of thermal efficiency is that it denotes the fraction of the heat in the stream that is recovered compared to the maximum heat transfer being thermodynamically feasible. The thermal efficiencies are physically bounded between zero and one, and the ratio between them is $P_{\mathrm{h}}/P_{\mathrm{c}} = CP_{\mathrm{c}}/CP_{\mathrm{h}}$. For ideal countercurrent flow, the expressions for P_{h} and P_{c} are as indicated in equations (3.13) and (3.14). Also, note that the thermal efficiencies are functions of flow configuration and NTU_{h} and NTU_{c}, only.

Using the thermal efficiencies, the correlation between the inlet and outlet temperatures of an ideal countercurrent heat exchanger is

$$\begin{bmatrix} T_{\mathrm{h,out}} \\ T_{\mathrm{c,out}} \end{bmatrix} = \begin{bmatrix} 1 - P_{\mathrm{h}} & P_{\mathrm{h}} \\ P_{\mathrm{c}} & 1 - P_{\mathrm{c}} \end{bmatrix} \begin{bmatrix} T_{\mathrm{h,in}} \\ T_{\mathrm{c,in}} \end{bmatrix} \tag{3.17}$$

This equation show that the relationship between inlet and outlet temperatures is linear. Considering *changes* in the inlet and outlet temperatures, the thermal efficiencies can be written as

$$P_{\mathrm{h}} = \frac{\Delta T_{\mathrm{h,out}}}{\Delta T_{\mathrm{c,in}}}, \quad P_{\mathrm{c}} = \frac{\Delta T_{\mathrm{c,out}}}{\Delta T_{\mathrm{h,in}}} \tag{3.18}$$

That is, an alternative interpretation of thermal efficiency is that it denotes the *gain* when an outlet temperature is affected by a change in the inlet temperature of the opposite stream. This implies that thermal efficiency, usually used in connection with design/sizing of heat exchangers, also have implications concerning control and operation of heat exchangers and HENs. For instance, the transfer matrix in equation (3.17) looses rank when $P_{\mathrm{h}} + P_{\mathrm{c}} = 1$, meaning that the outlet temperatures cannot be controlled *independently* using the inlet temperatures, see Mathisen (1994, chapter 3).

The temperature driving force in an ideal countercurrent heat exchanger is given by

$$\Delta T_{\mathrm{m}} = \begin{cases} \dfrac{(T_{\mathrm{h,in}} - T_{\mathrm{c,out}}) - (T_{\mathrm{h,out}} - T_{\mathrm{c,in}})}{\ln\left[(T_{\mathrm{h,in}} - T_{\mathrm{c,out}}) / (T_{\mathrm{h,out}} - T_{\mathrm{c,in}})\right]} & \text{when } CP_{\mathrm{h}} \neq CP_{\mathrm{c}} \\ (T_{\mathrm{h,in}} - T_{\mathrm{c,out}}) \quad \left(= (T_{\mathrm{h,out}} - T_{\mathrm{c,in}})\right) & \text{when } CP_{\mathrm{h}} = CP_{\mathrm{c}} \end{cases} \tag{3.19}$$

The upper part of this expression (when $CP_{\mathrm{h}} \neq CP_{\mathrm{c}}$) is the logarithmic mean temperature difference (LMTD), and it will be denoted ΔT_{lm}. The total heat transferred from hot to cold side of a heat exchanger can now be written in the simple form

$$Q = UA\Delta T_{\mathrm{m}} \tag{3.20}$$

The total heat transfer coefficient, U, is usually assumed to consist of three parts (the film theory); one filmcoefficient on the hot side (h_{h}), one filmcoefficient on the cold side (h_{c}) and one contribution from the heat conduction through the dividing wall given by k_{wall} and the geometry. For a flat wall with uniform thickness, l, and when neglecting geometrical effects near the edges, the total heat transfer coefficient is given by

$$\frac{1}{U} = \frac{1}{h_{\mathrm{h}}} + \frac{1}{h_{\mathrm{c}}} + \frac{l}{k_{\mathrm{wall}}} \tag{3.21}$$

The film coefficients are flow dependent, and estimates can be found using the Dittus-Boelter equation. This equation gives the Nusselt number ($Nu = hD/k$) as function of the Reynolds number and the Prandtl number. In the subsequent, the simulations are based on a specified total heat transfer coefficient, U, which is assumed to be independent of flow.

This section has given some basis for heat transfer, and the following section will utilize this for practical modeling of heat exchangers.

3.2 Dynamic model of a single heat exchanger

The type and complexity of the heat exchanger model greatly influences the time required and quality of the results from HEN simulations. The idea is to develop a general heat exchanger model consisting of a set of ordinary differential equations (ODE). Then, some standard simulation tool including an ODE-solver can be utilized for simulation. When heat exchangers are modeled, the basis is normally the mixing tank concept (lumped models/concentrated parameter models), *or* the distributed parameter models (partial differential equations) presented in the previous section. The presentation in this section aims at having elements from both these approaches. The three most important requirements for the general heat exchanger model are

1. The model should be simple.
2. Good agreement with steady state behavior of ideal countercurrent heat exchangers.
3. Fair agreement with the dynamic behavior of heat exchangers.

It will be necessary to simulate HENs with several units that may have heat load loops and controllers. Therefore, requirement 1 is crucial in order to simulate the complete HEN efficiently. It may be surprising that requirement 2 concern good agreement with *ideal* countercurrent heat exchangers instead of *real* heat exchangers. This is due to the importancy of comparing the results (at steady state) with the properties of the HEN from the early synthesis stage. At this stage, simple steady state models based on ideal countercurrent heat exchange (using LMTD) is normally used. The comparison with such models is considered most important when a method for operation is verified at a systems level. In practice, one should encourage that the simulations reflects the *real* HEN for the particular case, however, this requires decisions regarding heat exchanger types etc. to be taken in advance.

The following assumptions are made for the heat exchanger model:

- Constant densities of the two fluids.
- Constant specific heat capacities of the two fluids.
- Constant and flow independent heat transfer coefficient.
- No phase changes.

A countercurrent heat exchanger can be modeled from the assumption that each side consists of a series of ideal mixing tanks as shown in figure 3.2.

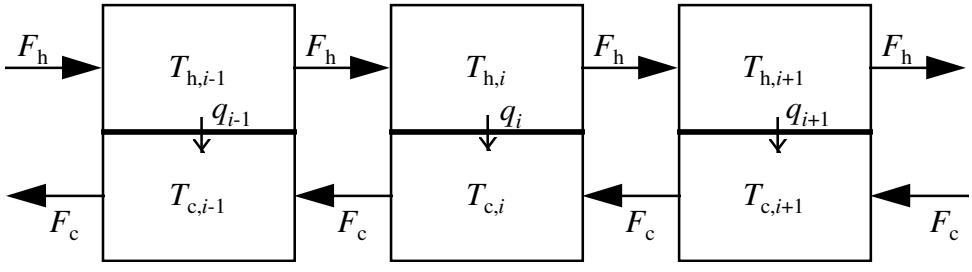

Figure 3.2 Sketch of mixing tank model.

The model for each stage becomes

$$\frac{\partial T_{\mathrm{h},i}}{\partial t} = \frac{F_{\mathrm{h}}}{V_{\mathrm{h},i}}\left(T_{\mathrm{h},i-1} - T_{\mathrm{h},i}\right) - \frac{UA_i}{\rho_{\mathrm{h}} V_{\mathrm{h},i} c_{\mathrm{v,h}}}\Delta T_{\mathrm{m},i} \tag{3.22}$$

$$\frac{\partial T_{\mathrm{c},i}}{\partial t} = \frac{F_{\mathrm{c}}}{V_{\mathrm{c},i}}\left(T_{\mathrm{c},i+1} - T_{\mathrm{c},i}\right) + \frac{UA_i}{\rho_{\mathrm{c}} V_{\mathrm{c},i} c_{\mathrm{v,c}}}\Delta T_{\mathrm{m},i} \tag{3.23}$$

where A_i is the heat exchanging area at stage i and $V_{\mathrm{h},i}$ and $V_{\mathrm{c},i}$ are the volumes of each compartment at hot and cold side. Numbering each stage from 1 to N, the heat exchanger model consists of $2N$ ordinary differential equations. At the inlet the boundary conditions are $T_{\mathrm{h},0} = T_{\mathrm{h,in}}$ and $T_{\mathrm{c},N+1} = T_{\mathrm{c,in}}$, and at the outlet we have $T_{\mathrm{h},N} = T_{\mathrm{h,out}}$ and $T_{\mathrm{h},1} = T_{\mathrm{c,out}}$.

The mixing tank concept can easily be modified to fit other configurations than countercurrent flow. Letting index i denote the hot side tank number and j the cold side tank number, the connection of hot and cold mixing tanks can be done by introducing a function $j = L(i)$. E.g. $j = L(i) = N + 1 - i$ results in a countercurrent configuration. This notation was introduced by Correa and Marchetti (1987), and the function L for some other configurations such as 1-2 shell-and-tube heat exchangers are given by Mathisen (1994, chapter 2, appendix 3). We will, however, assume countercurrent heat exchangers since this is normally assumed in the synthesis stage.

In equations (3.22) and (3.23), $\Delta T_{\mathrm{m},i}$ is the temperature driving force at stage i. Three alternatives (a, b and c) for this expression are:

a) Pure mixing tank model: $$\Delta T_{\mathrm{m},i} = T_{\mathrm{h},i} - T_{\mathrm{c},i} \tag{3.24a}$$

b) AMTD: $$\Delta T_{\mathrm{m},i} = 0.5\left[\left(T_{\mathrm{h},i-1} - T_{\mathrm{c},i}\right) + \left(T_{\mathrm{h},i} - T_{\mathrm{c},i+1}\right)\right] \tag{3.24b}$$

c) LMTD: $$\Delta T_{\mathrm{m},i} = \frac{\left(T_{\mathrm{h},i-1} - T_{\mathrm{c},i}\right) - \left(T_{\mathrm{h},i} - T_{\mathrm{c},i+1}\right)}{\ln\left[\left(T_{\mathrm{h},i-1} - T_{\mathrm{c},i}\right) / \left(T_{\mathrm{h},i} - T_{\mathrm{c},i+1}\right)\right]} \tag{3.24c}$$

The first alternative is the only option consistent with the *pure* mixing tank concept. The assumption of ideal mixing will underestimate the transferred heat at steady state since the driving forces are less than for ideal countercurrent flow. Using few stages, this may result in a considerable steady state error. In alternative *b*, the inlet temperatures at each stage are taken into consideration and the driving force is assumed to be the arithmetic mean of the temperature differences at each side of the stage. This compensates for the underestimation at steady state from the first alternative. Alternative *c* simply uses the LMTD which of course give perfect accordance with ideal countercurrent heat exchange at *steady state*. This option, however, may give serious problems in a dynamic simulation not only because it is undefined when the two temperature differences ($T_{\mathrm{h},i\text{-}1} - T_{\mathrm{c},i}$) and ($T_{\mathrm{h},i} - T_{\mathrm{c},i+1}$) are equal: In a dynamic simulation, it may for instance be a step in an inlet temperature resulting in crossover in the heat exchanger until steady state is reached. LMTD is derived for steady state, and with opposing temperature differences, it does not give any meaningful answer (since complex numbers have no physical interpretation in this case). Using LMTD in dynamic simulation

may easily abrupt an ongoing simulation and it is disregarded due to these problems. The Paterson approximation (Paterson, 1984) and the Chen approximation (Chen, 1987) are good approximations of the LMTD, developed to cope with the discontinuity of the LMTD for equal temperature differences. However, both of these approximations give the same problems as LMTD when crossover occurs (since they both involve the geometric mean), thus they are not suited for dynamic simulations.

Before proceeding, it will be shown that discretizing the partial differential equations (3.6) and (3.7) in the z-direction may result in *exactly* the same equations as in (3.22) and (3.23). Figure 3.3 shows control volumes and nodes on the hot and cold side along the z-axis.

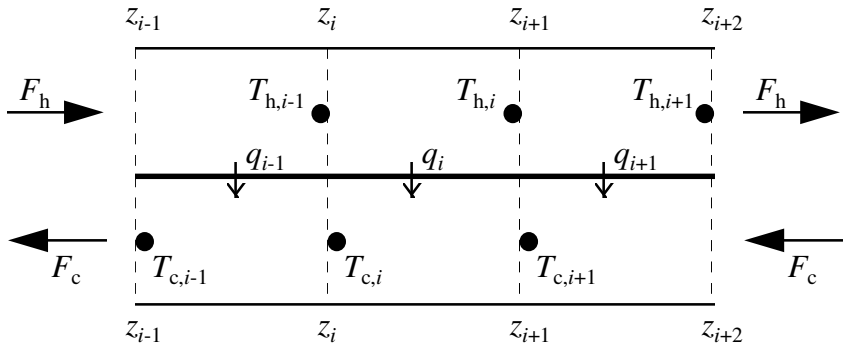

Figure 3.3 Illustration for discretization of equations (3.6) and (3.7).

As discretization method we will use a control volume approach to ensure that the energy balance is preserved for each control volume and not only within the total system boundaries, see Patankar (1980). Note that the nodes (marked with circular dots) are not located at the center of the control volumes, but are moved downstream to the "wall" of the each control volume. From equation (3.6) (the hot side) we obtain for control volume i:

$$\frac{\partial T_h}{\partial t}\int_{z_i}^{z_{i+1}}\partial z + \frac{F_h L}{V_h}\int_{T_{h,i-1}}^{T_{h,i}}\partial T_h = -\frac{UA}{\rho_h V_h c_{v,h}}\int_{z_i}^{z_{i+1}}(T_h - T_c)\partial z \tag{3.25}$$

According to figure 3.3, control volume i includes the region $i < z < i+1$. When z varies from i to $i+1$, T_h varies from $i-1$ to i due to the downstream shifting of the nodes. Hence, T_h is integrated from $i-1$ to i in equation (3.25). Performing the two first integrations, the equation can be written as

$$\frac{\partial T_h}{\partial t} + \frac{F_h}{V_h\frac{\Delta z}{L}}\left(T_{h,i} - T_{h,i-1}\right) = -\frac{UA}{\rho_h V_h c_{v,h}}\underbrace{\frac{1}{\Delta z}\int_{z_i}^{z_{i+1}}(T_h - T_c)\partial z}_{\Delta T_{m,i}} \tag{3.26}$$

Now, recognizing that $V_{h,i} = V_h \Delta z/L$ (similarly for cold side) and $A_{h,i} = A_h \Delta z/L$, and doing similar for the cold side (integrating T_c from i to $i + 1$) we obtain

$$\frac{\partial T_{\mathrm{h},i}}{\partial t} = \frac{F_{\mathrm{h}}}{V_{\mathrm{h},i}}\left(T_{\mathrm{h},i-1} - T_{\mathrm{h},i}\right) - \frac{UA_i}{\rho_{\mathrm{h}} V_{\mathrm{h},i} c_{\mathrm{v,h}}} \Delta T_{\mathrm{m},i} \tag{3.27}$$

$$\frac{\partial T_{\mathrm{c},i}}{\partial t} = \frac{F_{\mathrm{c}}}{V_{\mathrm{c},i}}\left(T_{\mathrm{c},i+1} - T_{\mathrm{c},i}\right) + \frac{UA_i}{\rho_{\mathrm{c}} V_{\mathrm{c},i} c_{\mathrm{v,c}}} \Delta T_{\mathrm{m},i} \tag{3.28}$$

which are identical to equations (3.22) and (3.23) found from the mixing tank concept. Assuming that the temperature in control volume i is constant and equal to $T_{\mathrm{h},i}$ on the hot side and $T_{\mathrm{c},i}$ on the cold side, $\Delta T_{\mathrm{m},i}$ from equation (3.26) becomes identical to alternative *a* in equation (3.24) (pure mixing tank). This assumption leads to discrete jumps in temperature from one control volume to the next. To be more realistic, one may assume the temperature to vary *linearly* between the nodes. Then, integrating $\Delta T_{\mathrm{m},i}$ in equation (3.26) results in AMTD as in alternative *b* in equation (3.24). Finally, one may assume the temperature variations between the nodes to follow the expressions in equations (3.13) and (3.14) which results in using LMTD (which we have decided to disregard).

To conclude so far, the modeling of a heat exchanger using the mixing tank concept, or discretizing the governing partial differential equations may result in identical sets of ordinary differential equations (provided the number of mixing tanks is equal to the number of control volumes, and the total volume and total area is divided into parts of equal size). It remains to (1) select a typical number of mixing tanks/control volumes, (2) select which of the alternatives *a* or *b* (from equation 3.24) should be used as mean temperature difference, and (3) select how bypass manipulations should be implemented. In the following, the mixing tanks and control volumes will be denoted "cells" as a common term. The number of cells is the number of tanks/volumes at each side.

Mathisen (1994, chapter 2) recommends a minimum of two cells in the pure mixing tank concept and minimum three cells when LMTD is used for dynamic purposes. Steady state considerations may give a higher bound on the minimum number of cells, particularly for the *pure* mixing tank concept. One way to compensate for the underestimation of the transferred heat is to increase the heat transfer coefficient. For *equal heat capacity flowrates* and N number of cells, the heat transfer coefficient has to be increased by the following ratio (Domingos, 1969).

$$\frac{U}{U_{\mathrm{lm}}} = \frac{N}{N - NTU_{\mathrm{lm}}} \tag{3.29}$$

where $NTU_{\mathrm{lm}} = U_{\mathrm{lm}}\mathrm{A}/CP$. Mathisen (1994, chapter 2) recommends a minimum number of cells for steady state considerations to be at least equal to NTU_{lm}. This is a rather loose bound since U approaches infinity when N approaches NTU_{lm}. If one requires the error in the pure lumped model to be less than 10%, this implies $N \geq 11NTU_{\mathrm{lm}}$. Also, the increase of U is dependent on the operating point when the heat capacity flowrates are different from each other. As a practical example, consider heat exchanger II in figure 2.4. Using a pure mixing tank model with four cells, U has to be increased by 94% in order to transfer the same heat as the steady state model in the nominal case. If $T_{\mathrm{s}}^{\mathrm{H1}}$ is decreased by 20°C, the increase in U should be almost four times. If only three cells are used, the increase is more than 180% in

the nominal case, and when T_s^{H1} is decreased by 20°C the duty will be too small even if U is infinite.

Using AMTD instead, the steady state error is much smaller. The relative error in transferred heat caused by AMTD (compared to LMTD) is given by

$$\frac{\text{AMTD} - \text{LMTD}}{\text{LMTD}} = \frac{0.5(\Delta T_2 / \Delta T_1 + 1)}{\Delta T_2 / \Delta T_1 - 1} \ln\left(\frac{\Delta T_2}{\Delta T_1}\right) - 1 \tag{3.30}$$

where ΔT_1 and ΔT_2 are the temperature differences between the hot and cold fluid at each side of the heat exchanger. The error is a function of the variable ($\Delta T_2/\Delta T_1$) only, and figure 3.4 shows the error.

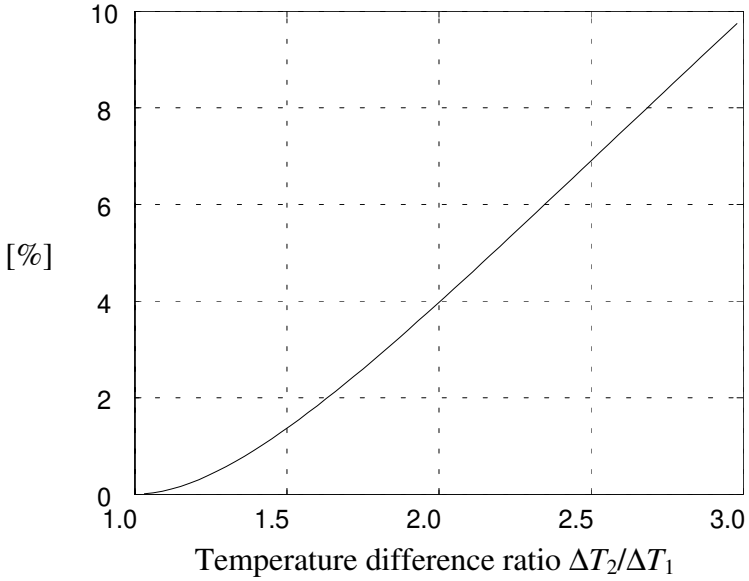

Figure 3.4 Relative error (in %) using AMTD compared to LMTD.

The error in a complete heat exchanger will be reduced as the number of cells increases since the parameter $\Delta T_2/\Delta T_1$ will approach 1 for each cell. This is the case also for the pure mixing tank model, but for AMTD the steady state error is much smaller for the same number of cells. To compare, U in heat exchanger II in figure 2.4 should be modified (reduced) by only 3.5% using AMTD and four cells (compared to 94% increase for the pure mixing tank model). Without any modifications, T_o^{C2} is only 0.5°C above correct value (i.e. using LMTD), and this is acceptable.

To achieve good agreement with the LMTD based models used in HEN synthesis, most simulations in this thesis have been carried out using AMTD and four cells (on each side) in the model. Heat transfer coefficients have not been modified. There is, however, a risk using AMTD as pointed out by Sangro (1996): While the pure mixing tank model underestimates the duty, the use of AMTD *overestimates* the duty compared to LMTD. Since LMTD origins from ideal countercurrent heat exchange, and since this is known to be the most effective configuration, AMTD will give a steady state duty slightly above the maximum possible theoretically. In most cases, this will not have any practical implications when comparing the simulations results with the models used during design. In some cases, however, the use of

AMTD may lead to crossover at steady state. This can occur when there are large differences in the heat capacity flowrates of the two fluids, and this very unphysical behavior of the models may give severe error in the simulation of a HEN. When simulating HENs using AMTD based models, it is important to verify that the error from equation (3.30) is acceptable for each heat exchanger and for all variations (in disturbances, parameters etc.) that may be encountered during the complete simulation.

Mathisen (1994, chapter 2) points out that wall dynamics should be included in many cases also for liquid heat exchangers. This may be important in order to have a correct response in outlet temperature due to changes in the inlet temperature of the opposite fluid. Despite this, wall dynamics is not included in the models used for simulation in this thesis. The reasons for this are (1) to have simple models (this was the first requirement stated at the beginning of this section) and (2) it is assumed that the dynamics of a *complete* HEN usually will not change significantly if dynamics of the dividing wall is neglected.

In order to simulate controlled HENs it is required to somehow incorporate variable bypass fractions. This is implemented directly into the heat exchanger model. The variable u denotes the fraction of the inlet stream being bypassed the heat exchanger on hot or cold side, and the stream actually flowing through the unit is $CP = (1-u)CP_{\text{in}}$. The outlet temperature after mixing is

$$T_{\text{out}} = uT_{\text{in}} + (1-u)\hat{T}_{\text{out}} \tag{3.31}$$

where $\hat{T}_{\text{out}}$ is the outlet temperature of the heat exchanger prior to mixing with the bypass stream.

In order to simplify the simulations and to reduce the risk of errors, it is important to specify few parameters for each heat exchanger in a HEN. This is achieved by specifying a nominal heat transfer coefficient (of 400W/°Km^2) and a nominal specific area (of 80m^2/m^3). Further, it is assumed that the volumes on hot and cold side are equal (nominally). Now, specifying UA, the area and volumes are easily calculated and hence a reasonable heat exchanger model is found by specifying only one parameter. UA for each heat exchanger is available from the early phase synthesis stage, and dynamic simulations can be carried out without the need for any more detailed decisions.

To summarize, the general heat exchanger model assumes incompressible flow (liquids), flow independant heat transfer coefficient, and it consists of four cells in a countercurrent configuration. The heat transfer from hot to cold side of each cell is found using arithmetic mean temperature difference and this corresponds to assuming linear temperature variations (streamwise) within each cell. A variable bypass is included in the general model.

3.3 Dynamic simulation of HENs

This section will show how the general heat exchanger model is used for simulation of HENs. The simulations are carried out using SIMULINK which is an extension of the MATLAB programming language. SIMULINK has a graphical user interface and it includes various solvers for sets of ordinary differential equations. The reasons for choosing SIMULINK were

mainly the graphical interface making it simple to generate new network structures and the additional ODE-solvers supplied with SIMULINK which turned out to be sufficient for HEN simulation

The heat exchanger model described in the last section is implemented as an S-function (see SIMULINK User's guide) which simply is an MATLAB function written in a format that SIMULINK can use as a *block*. A HEN is created simply by using the mouse to "drag-and-drop" blocks and lines between blocks. The SIMULINK representation of the HEN in figure 2.4 may take the form as shown in figure 3.5.

The HEN structure is easily recognized in figure 3.5 with the process streams represented by the wide lines. Stream H1 is defined with an inlet temperature of 190°C and *CP* equal to 100kW/°K. The Mux ("multiplexer") block H1 simply stacks the two input signals into one vector signal. The heat exchanger block "hxl_I" (which contains the general heat exchanger model) has four inputs where the two in the middle are the hot and cold inlet stream. The upper input of the heat exchanger blocks is the hot side bypass fraction and the lower input is the cold side bypass fraction. Thus, the actual heat exchanger implementation has bypasses on both hot and cold side making it more general. An unconnected input automatically takes the value of zero, meaning that the bypass is not used. The step blocks in figure 3.5 are for investigation of the responses due to steps in the bypass fraction of the hot side of heat exchanger I and the cold side of heat exchanger II. The two outputs in the middle from the heat exchanger blocks are the hot and cold outlet streams. These include one signal for the outlet temperature computed by the model and one signal for the *CP*-value. The *CP*-value is fed directly from the input to the output of the heat exchanger block, providing information to the next downstream heat exchanger. The upper and lower outputs from the heat exchanger blocks are dummies. The ability to rotate and flip blocks in SIMULINK makes it possible to draw the cold streams from right to left as shown in figure 3.5. This allows the HENs to be drawn in the countercurrent configuration quite similar to the grid diagrams, and this is important to easily verify that the simulated HEN structure is correct.

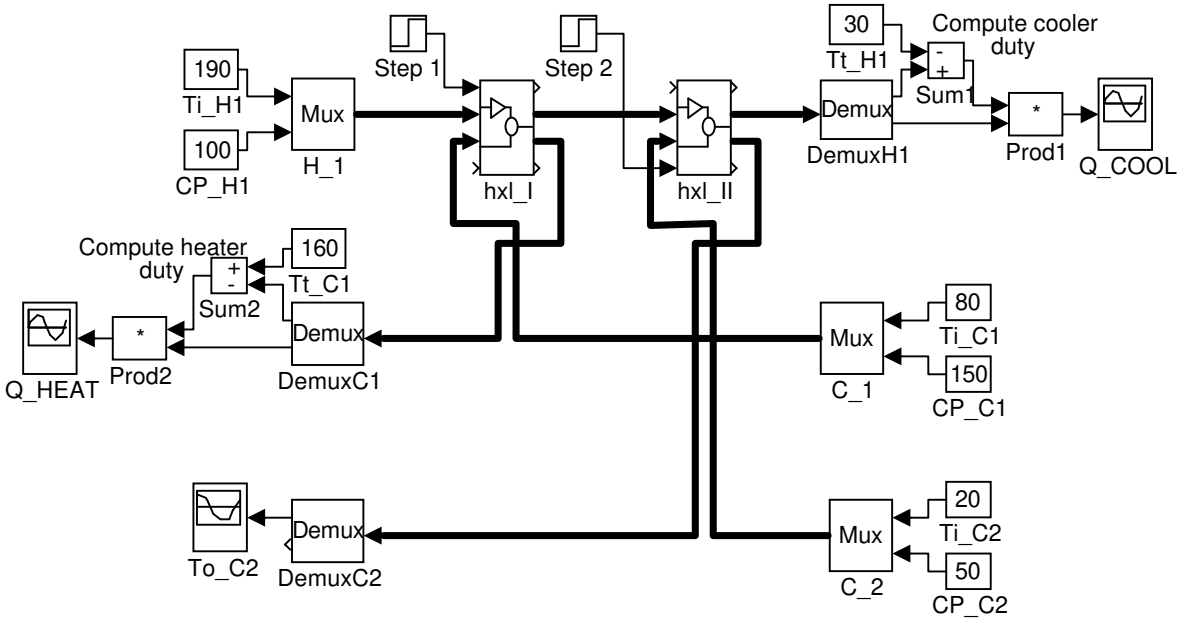

Figure 3.5 SIMULINK representation of a simple HEN.

One conspicuous feature of the HEN figure 3.5 compared to the grid diagram in figure 2.4 is the absence of the cooler and the heater. Recalling the decomposition rule for HENs from section 2.3 (Rule 2.1), the most important features of a HEN can be found from studying the responses in the bypass controlled outlet temperatures in addition to the utility consumption (assuming perfect control of the utility controlled outputs). This is exactly what is done in the upper right part of figure 3.5: The hot outlet temperature of heat exchanger II (upper output signal from the demultiplexer, "DemuxH1") is subtracted from the target temperature (30°C) and multiplied by CP_{H1} (lower output from "DemuxH1"). This is actually equation (2.4) shown graphically, and the result (cooler duty), is displayed during simulation by means of the "Auto-Scale Graph" block "Q_COOL". Similar calculations are done for stream C1 and "Q_HEAT" displays the heater duty. In this way, the bypass controlled outlet temperature together with the utility duties of the HEN can be investigated dynamically involving only two heat transferring units as opposed to the four units of the complete HEN. As a consequence, using the decomposition principle for simulation of HENs, modeling of final utility exchangers are completely avoided and the complexity of the simulations is significantly reduced.

SIMULINK (version 1.3) includes ODE-solvers (integrators) using methods such as an fifth order Runge-Kutta, Gear's method (for stiff systems) and an Adam's method. All of the algorithms uses variable step-lengths. A switch can be set to automatically choose Gear's method or Adam's method, depending on the stiffness, however, the manual advises against using these methods on discontinuous systems. A method denoted *linsim* is recommended by the manual for systems being relatively linear. The manual is economical on information about this method, except that it extracts the linear dynamics of a system, leaving only the nonlinear part to be simulated. Tests on all algorithms supplied with SIMULINK (version 1.3) have shown that the *linsim* algorithm performed best on simulation of HENs modeled as described in the previous section. Therefore, this algorithm is used for obtaining the results shown in this thesis.

3.4 Dynamic simulation of controlled HENs

As it was clear from chapter 2, most methods in this thesis will be based on decentralized control, and only simple controllers will be used (PI). A controller can be implemented as an S-function (as for the heat exchanger model) and a temperature can be "measured" simply by dragging a line from the process stream to the controller. Figure 3.6 shows the SIMULINK representation of the HEN in figure 5.5 when the control strategy proposed in chapter 5 is implemented.

In this case, the utility duties are not computed by SIMULINK during the simulation, but the inlet temperatures to the final utility exchangers are stored, and the utility duties are computed off-line using a simple MATLAB code. In figure 3.6, the outlet temperature of stream C1 is controlled by the bypass fractions across heat exchangers I, III and IV. The controller block actually contains three SISO-controllers where only one is active at a time. (The control strategy is explained in chapter 5).

Simulation of controlled HENs (using SIMULINK) will often introduce a problem usually not encountered by passive HENs. When the bypass of a manipulated bypass directly affects the outlet temperature (no dynamics) and the proportional part of the controller directly effects the bypass fraction when the measured temperature changes, an *algebraic loop* is introduced in the system. That is, the system is no longer a set of ordinary differential equations, but it is a set of *differential-algebraic* equations (DAE). SIMULINK does not include any efficient algorithms for solving DAE-systems, and iteration is performed at each time step to find a feasible solution. A possible way to change the DAE-system into a set of ODE, is to include some dynamics in the algebraic loops. For HENs, this may be done by introducing a small volume to represent energy hold-up in the bypass line. If this volume is selected too small, the system will become unnecessary stiff, and if the volume is selected too large, it may significantly affect the overall dynamics of the controlled HEN. For simulation results presented in this thesis, the volume of the bypass line is selected to be 20% of the total heat exchanger volume. Now, using equation (3.31) for mixing the bypass stream with the exit stream of the heat exchanger, the variable T_{in} has to be replaced by the temperature in the bypass mixing tank.

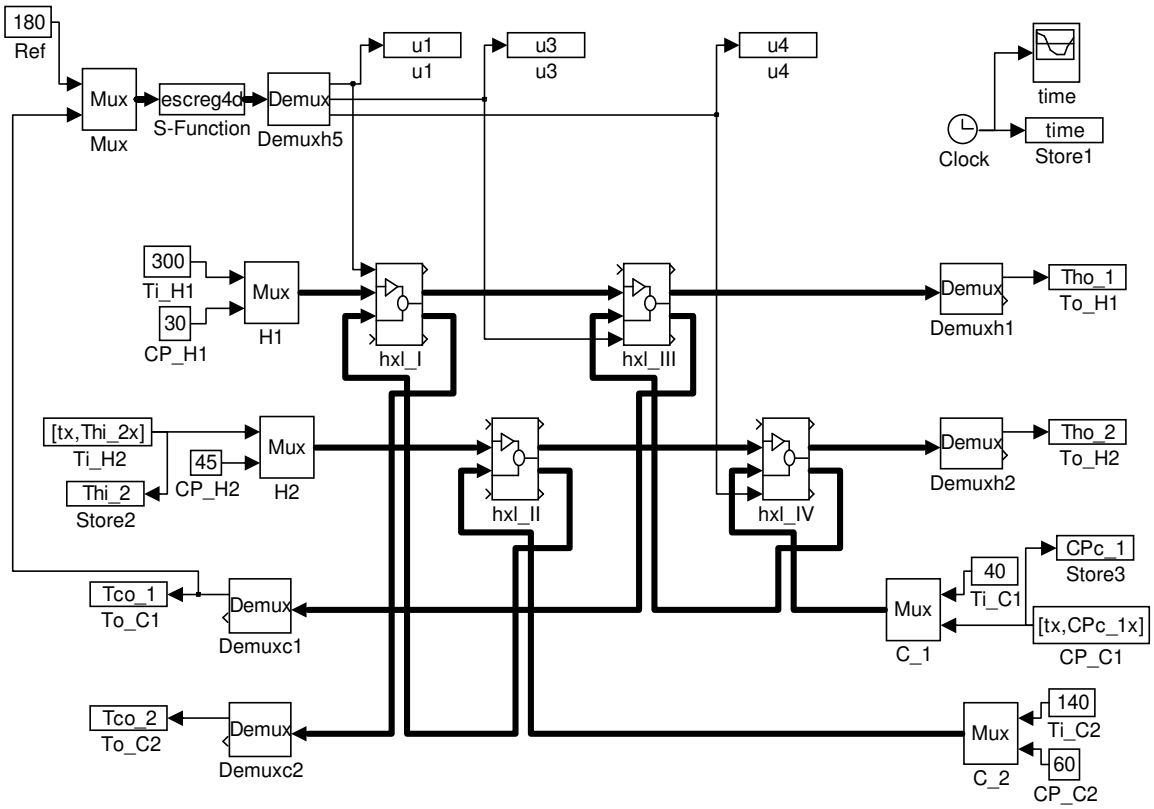

Figure 3.6 SIMULINK representation of a controlled HEN.

The method proposed in chapter 7 involves a steady state optimization to be carried out at periodic time intervals. This is also easily incorporated since all MATLAB functions are available in SIMULINK. The method is implemented by creating a SIMULINK block that utilizes the optimization functions in the MATLAB Optimization Toolbox.

3.5 Conclusions

The aim of this chapter has been to explain how the dynamic simulation results shown in this thesis are obtained. The main goal has been to develop models and use a simulation tool that make the simulations as easy to perform as possible, while retaining the essential properties of the HENs. In addition, some basic steady state properties of ideal countercurrent heat exchange has been shown.

The simulation of HENs is based on a simple heat exchanger model consisting of a set of ordinary differential equations. It has been shown that the particular model can be derived from the mixing tank concept, or from simplifying and discretizing the governing equation for heat transfer. Using arithmetic mean temperature difference in the mixing tank concept corresponds to assuming linear temperature variations between the nodes in the second approach.

In the literature on dynamic modeling of heat exchangers and HENs, the mixing tank concept (lumped models) and the distributed parameter models (based on partial differential equations) are often considered as two completely different approaches. In the description in this chapter, it has been tried to include both these approaches. It has been demonstrated that the two different approaches may result in exactly the same mathematical model.

Notation

A	Heat transfer area [m^2]
CP	Heat capacity flowrate [W/°K]
c_v	Specific heat capacity [J/(°Kkg)]
D	Diameter [m]
$\hat{E}$	Energy [J/kg]
$\hat{E}^U$	Internal energy [J/kg]
F	Volumetric flowrate [m^3/s]
h	Film coefficient for heat transfer [W/(°Km^2)]
k	Thermal conductivity. Dimensions may vary, but are often [W/(°Km)]
NTU	Number of transfer units [−]
q	Heat transferred from hot to cold side of each mixing tank/control volume [J]
Q	Total heat transferred from hot to cold side [J]
T	Temperature [°C]
U	Heat transfer coefficient [W/(°Km^2)]
UA	Heat transfer coefficient times area [W/°K]
V	Volume [m^3]

Subscripts

c	Cold
h	Hot
i	Index for mixing tank / control volume / temperature node, and index for velocities and positions using tensor notation (eq. 3.1).
lm	Logarithmic mean

m Mean (does not imply any specific averaging method)
o Outlet
s Supply

Greek

α Thermal diffusivity [m^2/s]
ΔT Temperature difference [°K]
ρ Density [kg/m^3]

References

Bird, R.B., W.E. Stewart and E.N. Lightfoot (1960). *Transport Phenomena*. John Wiley & Sons, Singapore.

Chen, J.J.J. (1987). Letter to editors. Comments on a Replacement for the Log-arithemic Mean. *Chem. Eng. Sci.*, **42**, 2488.

Correa, D.J. and J.L. Marchetti (1987). Dynamic Simulation of Shell-and-Tube Heat Exchangers. *Heat Transfer Eng.*, **8**, 50.

Domingos, J.D. (1969). Analysis of Complex Assemblies of Heat Exchangers. *Int. Journal of Heat Mass Transfer.*, **12**, 537.

Mathisen, K.W. (1994). Integrated Design and Control of Heat Exchanger Networks. *Ph.D. Thesis*. University of Trondheim - NTH, Norway.

Patankar, S.V. (1980). *Numerical Heat Transfer and Fluid Flow*. Hemisphere Publishing Corp., USA.

Paterson, W.R. (1984). A Replacement for the Logarithmic Mean. *Chem. Eng. Sci.*, **39**, 1635.

Sangro, K.I. (1996). Models for Dynamic Simulation of Heat Exchanger Networks. *Diploma Thesis* (in Norwegian). Telemark Institute of Technology, Porsgrunn, Norway.

Sha, W.T., C.I. Yang, T.T. Kao and S.M. Cho (1982). Multidimensional Numerical Modeling of Heat Exchangers. *Journal of Heat Transfer*, **104**, 417.

SIMULINK User's Guide (1992). The MathWorks Inc., Massachusetts, USA.